Surface ozone-temperature relationships in the eastern US: A monthly climatology for evaluating chemistry-climate models

D.J. Rasmussen[a], A.M. Fiore[a], V. Naik[b], L.W. Horowitz[a], S.J. McGinnis[c], M.G. Schultz[d]

a. Geophysical Fluid Dynamics Laboratory (GFDL), National Oceanic and Atmospheric Administration (NOAA), Princeton, New Jersey 08540, USA.
b. High Performance Technologies Inc./GFDL, NOAA, Princeton, New Jersey 08540, USA.
c. Department of Geosciences, Princeton University, Princeton, New Jersey 08544, USA.
d. IEK-8, Forschungszentrum Jülich, Jülich, Germany.

***Corresponding author:**
D.J. Rasmussen (david.rasmussen@noaa.gov)

Abstract.

We describe a mechanistic approach to model evaluation that seeks to characterize pollutant sensitivity to year-to-year fluctuations in weather, motivated by the hypothesis that our approach offers a good observational basis for assessing model skill at projecting air quality response to changes in climate. We first produce a monthly climatology of the surface ozone (O_3)-temperature relationship ($d[O_3]/dT$) using monthly averages of daily maximum surface temperature (T_{max}) and of maximum daily 8-hour average (MDA8) O_3 from the US Environmental Protection Agency Clean Air Status and Trends Network (CASTNet) over the eastern US from 1988 through 2009. The CASTNet is designed to characterize conditions that are representative of the regional scale. We define $m_{O3\text{-}T}$ as the slope of the best fit line between monthly average values of MDA8 O_3 and of daily T_{max} for each year. Applying two distinct statistical approaches to aggregate local measurements to the regional scale, we find that summertime $m_{O3\text{-}T}$ is 3–6 ppb K^{-1} (r = 0.5–0.8) over the Northeast, 3–4 ppb K^{-1} (r = 0.5–0.9) over the Great Lakes, and 3–6 ppb K^{-1} (r = 0.2–0.8) over the Mid-Atlantic. By separating our analysis into two periods, 1988–1999 and 2000–2009, we confirm the previously noted decrease of roughly 1 ppb K^{-1} in $m_{O3\text{-}T}$ driven by NO_x emission reductions from eastern US power plants

in the late 1990s and early 2000s (Bloomer et al., 2009). We then evaluate the ability of the Geophysical Fluid Dynamics Laboratory (GFDL) Atmospheric Model version 3 (AM3), a global chemistry-climate model (CCM), to resolve the observation-derived O_3-temperature relationship. The model captures the general features of the seasonal variations in correlation coefficients and $m_{O3\text{-}T}$ despite biases in both monthly mean summertime MDA8 O_3 (up to +10 to +30 ppb) and daily T_{max} (up to +5 K) over the eastern US. We show that the model reproduces $m_{O3\text{-}T}$ for the Northeast ($m_{O3\text{-}T}$= 2–6 ppb K^{-1}; r = 0.6–0.9), although it severely underestimates $m_{O3\text{-}T}$ by 4 ppb K^{-1} in some summer months over the Mid-Atlantic, in part due to excessively warm temperatures above which O_3 production saturates in the model. Combining modeled T_{max} biases with a conservative observation-based $m_{O3\text{-}T}$ estimate of 3 ppb K^{-1} we find that modeled temperature biases may explain as much as 5–15 ppb of the MDA8 O_3 bias in August and September, though cannot account for the majority of the bias. Long-term coincident measurements of air pollution and meteorological variables can provide constraints necessary to evaluate the ability of CCMs to capture the processes relevant to projecting future air quality response to changes in climate.

1. Introduction.

Surface ozone (O_3) is a secondary pollutant that is produced by the photochemical oxidation of carbon monoxide (CO), methane (CH_4), and non-methane volatile organic compounds (NMVOCs) by OH in the presence of nitrogen oxides ($NO_x \equiv NO + NO_2$). Observational studies have shown strong correlation between surface temperature and O_3 concentrations (Bloomer et al., 2009; Camalier et al., 2007; Cardelino and Chameides, 1990; Clark and Karl, 1982; Korsog and Wolff, 1991). It is widely anticipated that a warming climate will exacerbate O_3 pollution in densely populated regions of the US, such as over the Northeast where climate models consistently show annual temperature increases of at least 2 K over the 21st century (Christensen et al., 2007), by offsetting the benefits from emissions reductions, increasing the number of high-O_3 days, and lengthening the O_3 season (Bloomer et al., 2010; Hogrefe et al., 2004; Jacob and Winner, 2009; Kunkel et al., 2008; Murazaki and Hess, 2006; Nolte et al., 2008; Racherla and Adams, 2006; Wu et al., 2008). Increasing concentrations of surface O_3 resulting from climate change are a public health concern (Bernard et al., 2001; Levy et al., 2001). As such, air quality managers seek to be informed as to how surface O_3, among other pollutants, will evolve in the

63 future. Chemistry-climate models (CCMs) are increasingly being applied to project air quality
64 under various global change scenarios. These models, however, have known biases in their
65 simulations of present-day meteorology and chemical environments that raise concern as to their
66 ability to project accurately the response of air pollution to changes in climate (Fiore et al., 2009;
67 Murazaki and Hess, 2006; Reidmiller et al., 2009).
68
69 Here we assess the capacity of a CCM to represent the surface O_3 response to interannual
70 variations in temperature. We focus on this well-established correlation between O_3 and monthly
71 average temperatures in the warm season over the eastern US (Dawson et al., 2007; Lin et al.,
72 2001; National Research Council (U.S.). Committee on Tropospheric Ozone Formation and
73 Measurement., 1991; Sillman and Samson, 1995). While some studies solely compare simulated
74 and observed O_3 or temperature to gauge the abilities of a CCM, this evaluation should provide a
75 better indication of the ability of a CCM to resolve accurately the surface O_3 response to
76 projected climate change driven increases in average temperatures. Similar mechanistic air
77 quality model evaluation approaches have previously been applied to gauge the O_3 response to
78 simulated NO_x emission reductions over the eastern US (Gilliland et al., 2008; Godowitch et al.,
79 2008).
80
81 Temperature is a useful proxy to synthesize the complex effects of meteorological and chemical
82 factors influencing O_3 concentrations, and that these effects can be represented aggregately by a
83 total derivative ($d[O_3]/dT$) commonly thought to reflect at least three components in the eastern
84 US: (1) association of warm temperatures with stagnant air masses enabling accumulation of
85 local chemistry precursors that feed O_3 formation in the planetary boundary layer (Jacob et al.,
86 1993; Olszyna et al., 1997); (2) thermal decomposition of peroxyacetylnitrate (PAN) at high
87 temperatures, thus decreasing NO_x and HO_x sequestration at low temperatures (Cardelino and
88 Chameides, 1990; Sillman and Samson, 1995); and (3) increasing biogenic emissions of
89 isoprene, a major NMVOC precursor for O_3 formation under high-NO_x conditions (Guenther et
90 al., 1993; Lamb et al., 1987; Meleux et al., 2007)
91
92 Additional processes contribute to increasing O_3 with temperature with varying importance
93 across regions. These include: decreased ventilation by migratory cyclones in the Northeast as

stagnation events increase (Leibensperger et al., 2008) and wildfires in the western US. Anthropogenic and natural emissions of NO_x may also increase with temperature (Brühl and Crutzen, 1988; Logan, 1983; Yienger and Levy, 1995). Other temperature dependent processes have shown variable effects on O_3 concentrations such as humidity in the Mid-Atlantic (Camalier et al., 2007; Davis et al., 2011; Dawson et al., 2007) and mixing depths in southern California (Aw and Kleeman, 2003) and in the eastern US (Dawson et al., 2007; Rao et al., 2003). Here we focus on $d[O_3]/dT$, which can be determined from available long-term meteorology and underscore a need for future work to identify observed constraints on the individual processes (partial derivatives) contributing to $d[O_3]/dT$.

Past studies have found $d[O_3]/dT$ to be approximately linear over the temperature range of 290 – 305 K (Bloomer et al., 2009; Camalier et al., 2007; Mahmud et al., 2008; Sillman and Samson, 1995). The slope of this linear relationship, hereafter $m_{O3\text{-}T}$ (Steiner et al., 2010), has been referred to as the "climate change penalty factor" (Bloomer et al., 2009) in reference to the increase in O_3 associated with increasing temperature. Using the climate penalty factor to project historical relationships into the future assumes stationarity in chemical environments (e.g. emissions of both anthropogenic and biogenic origin) and neglects known complex chemistry-weather feedbacks (Lin et al., 1988; National Research Council (U.S.). Committee on Tropospheric Ozone Formation and Measurement., 1991; Steiner et al., 2006; Weaver et al., 2009). We suggest that a more informative application of an observationally derived $m_{O3\text{-}T}$ lies in its utility for assessing the skill of CCMs to reproduce historical O_3-temperature relationships. A proportionate amount of confidence can then be applied to estimates of any "climate change penalty" calculated by the CCM. This climate change penalty has been previously defined equivalently within the context of both O_3 and NO_x: (a) the reduced benefits of emission controls due to the increase in O_3 in a warmer climate; (b) the additional decreases in NO_x emissions needed to counter any climate-induced increase in O_3 in order to meet established air quality goals (Wu et al., 2008).

Since a global CCM is expected to resolve synoptic, though not local, scales (e.g. Fiore et al., 2003), we construct regional O_3-temperature climatologies in the eastern US where pollution episodes are large-scale (Logan, 1989) and observational records are longest. Significant spatial

and temporal variability in the O_3-temperature relationship has been found across the eastern US due to variations in chemical and meteorological environments that strongly influence surface O_3 formation (Bloomer et al., 2010; Camalier et al., 2007; Jacob et al., 1995; Klonecki and Levy, 1997). Due to differences between urban and rural O_3-temperature sensitivities (Sillman and Samson, 1995), we anticipate that some sub-regional scale emissions and meteorology patterns may complicate characterization of broad spatial patterns in these relationships.

We use 22 years of temperature and surface O_3 observations (1988–2009) from the US Environmental Protection Agency (EPA) Clean Air Status and Trends Network (CASTNet; http://www.epa.gov/castnet) and a 20-year simulation (1981–2000) from the atmosphere component, the Atmospheric Model version 3 (AM3), of the Geophysical Fluid Dynamics Laboratory (GFDL) coupled general circulation model version 3 (CM3) (Donner et al., 2011; Naik et al., in prep), and our statistical approach (Section 2). We then present a climatology of monthly O_3-temperature relationships constructed from observations at both site-level and regional scales, and assess whether our approach reveals the roughly 1 ppb K^{-1} regionally observed decrease in $m_{O3\text{-}T}$ that has been previously attributed to the NO_x State Implementation Plan (SIP) Call in late 1990s and early 2000s which reduced power plant NO_x emissions during the O_3 season (Bloomer et al., 2009) (Sect. 3). These observation-based climatologies are then used to evaluate the GFDL AM3 CCM (Sect. 4). Finally, we apply the observed O_3-temperature relationships to quantify any contribution from AM3 temperature biases in the eastern US to the summertime AM3 O_3 bias, which has also been noted in present day regional (Nolte et al., 2008) and global (Fiore et al., 2009; Murazaki and Hess, 2006; Reidmiller et al., 2009) chemical transport models (Sect. 5), and conclude (Sect. 6).

2. Datasets and Statistical Approach.

2.1 CASTNet observations

Operating since 1987, the CASTNet (Clarke et al., 1997) is an observational network that is spatially designed to be regionally representative of rural conditions[1], potentially more suitable to compare with a coarse horizontal resolution (in this case, roughly 2^o) global climate model

[1] EPA, CASTNet Facts Sheet; http://epa.gov/castnet/javaweb/docs/CASTNET_factsheet_2007.pdf

than other available datasets. The CASTNet measures both pollutants and weather variables; we use co-located, hourly surface O_3 and temperature. Temperature is at 2-m, measured with platinum resistance (accuracy, ± 0.5 K; precision, ± 1.0 K) and O_3 with ultra-violet absorbance (accuracy and precision, ± 10%)[2]. We use monthly mean maximum daily surface temperature (herein denoted as T_{max}) and monthly mean maximum daily 8-hour average (MDA8) O_3 calculated from hourly observations, requiring at least 20 days of data per month. Each of these 20 days must have at least 18 hourly temperature and O_3 values in addition to 6 out of 8 hourly O_3 observations to calculate an 8-hour O_3 average.

2.2 Model Description.

The GFDL AM3 CCM includes fully coupled stratospheric and tropospheric (both aerosol and NO_x-hydrocarbon-O_3) chemistry and aerosol-cloud interactions within a general circulation model (GCM). As described in detail by Donner et al. (2011), AM3 includes several new physical parameterizations relative to the previous generation (AM2) models and is coupled to a land model (LM3) that includes dynamic vegetation and hydrology (Shevliakova et al., 2009). The tropospheric chemistry and stratospheric chemistry derive from MOZART-2 (Horowitz et al., 2003) and AMTRAC (Austin and Wilson, 2006), respectively, as described fully by Naik et al. (in prep) who evaluate global trace gas distributions over recent decades with in situ measurements.

The dynamical core for AM3 is finite-volume, implemented on a cubed sphere (Putman and Lin, 2007). The native cubed sphere grid is C48 horizontal resolution (48 x 48 cells per face, with the size of the grid cell ranging from ~163 km at the corners to ~231 km near the face centers) and has 48 vertical layers (top level centered at 1.7 Pa). We analyze simulated hourly surface O_3 and hourly temperature fields that have been re-gridded to a latitude-longitude grid with 2° x 2.5° horizontal resolution.

[2] EPA, CASTNet Quality Assurance, 3rd Quarterly Report, 2010; http://epa.gov/castnet/javaweb/docs/QA_Quarterly_2010_Q3.pdf

Our simulation follows the specifications for the GFDL AM3 "AMIP" simulations for CMIP5 as described by Donner et al. (2011), except for interactive isoprene emissions as described below. Briefly, AM3 is driven with observed sea surface temperatures and sea ice (Rayner et al., 2003) and aerosol and O_3 precursor emissions from the Atmospheric Chemistry and Climate Model Intercomparison Project (ACCMIP) historical dataset (Lamarque et al., 2010). Thus, we do not expect the model to correspond to the actual synoptic meteorology during the simulation period; certain aspects of interannual variability (those not forced by sea surface temperatures) will not be captured by the model. Greenhouse gas concentrations are set to spatially uniform values for radiation (Meinshausen et al., 2011); for chemically reactive species, those values are additionally applied as lower boundary conditions. We conduct a 21-year simulation, from 1980–2000, and analyze results from 1981–2000 to allow for a one-year initialization. We find little change in eastern U.S. (bounded by 60^o W–95^o W and 25^o N–50^o N) surface anthropogenic NO_x emissions over this period, with annual emissions of 4.23, 4.40, and 4.29 Tg N yr^{-1} in 1980, 1990, and 2000, respectively. Given the small magnitude of these changes, we expect the O_3-temperature relationship to reflect weather variability in the model over these two decades rather than the O_3 response to changes in NO_x emissions.

In order to allow isoprene emissions to respond to fluctuations in solar radiation and temperature, we implement a version of Model of Emissions of Gases and Aerosols from Nature (MEGAN) (Guenther et al., 2006), following the approach used in MOZART-4 (Emmons et al., 2010). Emission capacities for five vegetation types are included (version 2.1). Global distributions of 17 plant functional types (PFT) and corresponding leaf area index are based on AVHRR and MODIS data, as used in the NCAR Community Land Model (CLM) (Lawrence and Chase, 2007) and mapped to the five MEGAN vegetation types (see Table 8 of Emmons et al., 2010). Note that these vegetation types and leaf area indices are independent of those within the LM3 by the dynamic vegetation model. Our implementation uses the model surface air temperature and downward short-wave visible radiation flux each time step, and also includes a dependence on the observed climatological surface air temperature and total downward solar radiation from the previous month. These climatological fields are taken from Sheffield et al. (2006) and are averaged from 1980 to 2000 separately for each month. Annual isoprene emissions for our 1981–2000 period range from 368–405 Tg C globally, and 16–23 Tg C within the United States.

214

215 **2.3 Statistical Approach.**

216

217 We characterize O_3-temperature relationships by: (1) Pearson correlation coefficients (r) and (2)
218 the slope of the regression line ($m_{O3\text{-}T}$) calculated from monthly mean T_{max} and monthly mean
219 MDA8 O_3 from CASTNet and the GFDL AM3 CCM. The Spearman's rank correlation (Wilks,
220 2006), a non-parametric statistic (i.e. does not assume Gaussian characteristics), for all
221 correlation analyses yielded little numerical difference from the Pearson correlation coefficients.
222 For calculating $m_{O3\text{-}T}$, we use the reduced major axis (RMA) method, ideally suited for the
223 presence of measurement uncertainties in both x- and y- variables (Ayers, 2001; Cantrell, 2008;
224 Davis, 1986). Unless otherwise noted, all observed data are from 1988–1999, prior to the
225 implementation of the NO_x control SIP Call to avoid aliasing the impacts of NO_x emission
226 changes on O_3 into our estimate of the O_3 response to temperature (Frost et al., 2006; Gego et al.,
227 2008; Gego et al., 2007). This time period additionally aligns well with the model simulation
228 (1981–2000).

229

230 We estimate O_3-temperature relationships using three different groupings of monthly mean
231 CASTNet observations and model output for each month: (1) at individual CASTNet sites with
232 at least 7 years of data over the period of 1988–1999 and at sites below 600 meters to exclude
233 high-altitude measurements that are heavily influenced by free tropospheric air, with different
234 O_3-temperature relationships (Wunderli and Gehrig, 1991); (2) aggregating into three regions
235 (Figure 1) monthly mean data for all years, at all sites within a region that meet our selection
236 criteria; and (3) regionally averaged (across all sites meeting our selection criteria) monthly
237 means for all years.

238

239 Site groupings for the regional scale estimates are motivated by past statistical analyses (Chan,
240 2009; Eder et al., 1993; Lehman et al., 2004), with additional site selection criteria to include
241 only regionally representative sites. Criteria include: (1) site elevation must be below 600 meters
242 to avoid including free tropospheric air that is not representative of surface conditions, (2) sites
243 must be approximately 50 km from oceanfront to remove local land-sea meteorological effects,
244 and (3) sites must have data record lengths of at least seven years for each of the three periods

we analyze: 1988–1999, 2000–2009, or 1988–2009. We sample the model at the grid box that containing the site latitude and longitude. When more than one site fell within the same model grid box, the site with the longest observational record was used.

3. Observed monthly climatologies of the MDA8 O_3-T_{max} relationship.

3.1 Climatology for individual CASTNet sites in May and July.

We begin by assessing the relationships between MDA8 O_3 and T_{max} at individual CASTNet sites. Here we limit our evaluation to two months during the eastern US O_3 season: (1) May, during which we expect a seasonal transition in the photochemical environment controlling O_3 formation (e.g. changing solar zenith angles, photolysis rates, humidity, and biogenic VOC emissions) (Jacob et al., 1995; Kleinman, 1991; Klonecki and Levy, 1997) and (2) July, when maximum O_3 concentrations typically occur in the eastern US (Bloomer et al., 2010). The O_3-temperature correlations at each CASTNet site meeting the predefined selection criteria (Sect. 2.3) range from $r < 0$ to +0.9 in the Mid-Atlantic and generally increase with latitude to 0.3–0.9 in the Great Lakes and the Northeast regions in May (Figure 2a). This gradient is consistent with that found for a statistical model built on several meteorological variables (predominantly temperature and relative humidity; see Fig. 2, Davis et al., (2011)) A smaller range of 0.3–0.9 with no latitudinal trend is observed in July over the eastern US (Figure 3a).

Values of May and July $m_{O3\text{-}T}$ across individual CASTNet sites vary over the eastern US, however some regional spatial homogeneity occurs in the Great Lakes and Northeast regions in May ($m_{O3\text{-}T}$ = 1–3 ppb K^{-1}; Figure 2b). Observed May and July $m_{O3\text{-}T}$ tend to decrease with increasing latitude from 4–6 ppb K^{-1} in the southeastern US to 1–2 ppb K^{-1} in May and 2–3 ppb K^{-1} in July (Figure 3b) at the Ashland, Maine CASTNet site. This decrease in $m_{O3\text{-}T}$ from south to north also is consistent with the findings of Davis et al. (2011).

3.2 Seasonal variations in regional relationships between MDA8 O_3 and T_{max}.

We compile monthly mean MDA8 O_3 and T_{max} across all sites within each region (Figure 1) to construct regional relationships by month for the Northeast, Mid-Atlantic, and Great Lakes

(Figure 4). We consider two time periods: 1988–1999 as in Figures 2 and 3, as well as 2000–2009, to examine the impact of the 1998 NO_x SIP Call which reduced summertime power plant emissions in the eastern US by roughly 50% between 1999 and 2003 (Frost et al., 2006).

We first illustrate our approach by estimating $m_{O3\text{-}T}$ for July monthly mean MDA8 O_3 versus July mean T_{max} at each CASTNet site for each year during the period 1988–1999 (Figure 4). Strong linearity exists between daily T_{max} and MDA8 O_3 over the Northeast ($r = 0.7$; Figure 4a) and the Great Lakes ($r = 0.8$; Figure 4g), while a weaker relationship is present in the Mid-Atlantic ($r = 0.4$; Figure 4d).

Throughout the year we find that O_3-temperature correlations in the Mid-Atlantic (Figure 4e) are weakest in May, June, and July, ($r < 0.5$) and highest in the autumn, winter, and spring ($r = 0.6$–0.7). In contrast, O_3 and temperature are most strongly correlated in the warmer months in the Northeast (Figure 4b) and the Great Lakes ($r = 0.6$–0.7; Figure 4h), and anti-correlated during winter. Hot summer temperatures in the Mid-Atlantic region are not a reliably strong predictor of high levels of O_3, possibly reflecting offsetting effects of hot and cloudy conditions, a hypothesis previously put forth for the O_3-temperature relationship observed at a site in suburban Georgia (Cardelino and Chameides, 1990). Additionally, summer temperatures in the Mid-Atlantic may regularly exceed those known to induce an O_3 response, resulting in an O_3 production "plateau", which has been attributed to declining impacts of PAN decomposition at higher temperatures (Steiner et al., 2010).

In all regions, the observed $m_{O3\text{-}T}$ for 1988–1999 has a distinct seasonal cycle, with the highest sensitivities (3–6 ppb K^{-1}) present during the summer and early autumn (Figure 4c, f, and i). Mean $m_{O3\text{-}T}$ for the O_3 season matches well with the ~3 ppb K^{-1} calculated by Bloomer et al. (2009) over the Great Lakes, Northeast, and Mid-Atlantic. Furthermore, we find that a decrease of roughly 1 ppb K^{-1} in $m_{O3\text{-}T}$ during the O_3 season from 1988–1999 to 2000–2009 emerges, agreeing with the reductions found by the same Bloomer study (see Fig. 3, Bloomer et al., 2009).

We note an apparent discrepancy between the $m_{O3\text{-}T}$ in July in the Northeast at the individual CASTNet sites (2–6 ppb K^{-1} in Figure 3b) versus the 6 ppb K^{-1} in Figure 4c. Since Figure 4c

307 includes all the individual sites, we hypothesize that the larger slope reflects the spatial gradients
308 in the O_3 and T_{max} relationship across the region rather than a regionally enhanced O_3 response to
309 temperature. We next attempt to separate the influence of these spatial gradients from the impact
310 of year-to-year weather fluctuations on O_3. As a first step, we examine climatologies of July
311 monthly mean MDA8 O_3 and T_{max} at CASTNet sites over the eastern US in Figure 5. We find
312 large variability in the mean July MDA8 O_3 and T_{max} within each of the three regions, including
313 a strong dependence on latitude. In an attempt to filter out this spatial variability, we average the
314 MDA8 O_3 and T_{max} over all CASTNet sites in each region to create regional average records of
315 O_3 and temperature for each month within each year. Averaging only occurs when at least 75%
316 of the sites in each region (Figure 1) report data for that month. Given the scarcity of temporally
317 coincident observations from sites for the 1988–1999 period, we increase the sample size by
318 expanding to use the full record length of 1988–2009. We then use these regional averages, one
319 value per year, to estimate $m_{O3\text{-}T}$ for each month.
320
321 Using this method, the observed $m_{O3\text{-}T}$ and r-values in the both the Great Lakes and the Mid-
322 Atlantic are similar to those when we allow each site to contribute individually to the O_3-
323 temperature relationship (Figure 4 vs. Figure 6), indicating that the relationships in Figure 4
324 primarily reflect "climatic" variations of MDA8 O_3 with T_{max}. For a quantitative comparison, the
325 seasonality of $m_{O3\text{-}T}$ calculated with observations from 1988–2009 with the methodology used in
326 Figure 4 is presented as dashed lines (Figures 6c, f, and i). Over the Northeast, the two methods
327 yield differing values of $m_{O3\text{-}T}$ of up to 2 ppb K^{-1} (solid vs. dashed black lines in Figure 6c). The
328 lower July sensitivity in Figure 6c is more consistent with what one would calculate from
329 averaging the values of $m_{O3\text{-}T}$ at individual sites in the Northeast (Figure 3b). Even with the full
330 22-year record of CASTNet observations, the calculation of $m_{O3\text{-}T}$ produces standard errors of
331 roughly ± 1 ppb K^{-1} during the warmer months of the year—pointing to a need for longer
332 datasets to improve statistical power. These uncertainties highlight the importance of the
333 continued operation of quality controlled O_3 and temperature measurements in support of their
334 crucial role in delineating spatial and temporal patterns in relationships between air pollutants
335 and meteorology. Characterizing these relationships is vital for a mechanistic approach to CCM
336 evaluation.
337

4. Evaluating modeled climatologies of the MDA8 O_3-T_{max} relationship.

Here we compile results from a 20-year simulation with the GFDL AM3 CCM with our constructed climatology of O_3-temperature statistics in Section 3. Modeled and observed MDA8 O_3 and T_{max} are compared at individual sites in Figures 2 and 3. In May, the model (Figure 2c) captures the broad range of observed correlation coefficients from south to north ($r < 0$ to +0.9) over the eastern US (Figure 2a). North of roughly 37^o N, the model (Figure 2d) reproduces the range of observed $m_{O3\text{-}T}$ in May (Figure 2b), and the model (Figure 3d) generally captures the north-south gradients along the Eastern Seaboard in July (Figure 3b) where Camalier et al. (2007) found the highest observed response of O_3 to temperature over the eastern US. The high correlation between O_3 and temperature in summer (r = 0.3–0.9) is reproduced by the GFDL AM3 CCM only in the northern half of the domain (Figure 3c) and $m_{O3\text{-}T}$ is underestimated in the Mid-Atlantic US, particularly in the southern and central portions of the region, in May (Figure 2d) and July (Figure 3d).

We assess the GFDL AM3 CCM at the regional scale by compiling monthly mean MDA8 O_3 and T_{max} across all grid boxes that contain CASTNet sites to construct regional relationships by month (Figure 4). Here we compare the model simulation (1981–2000) to the observation period prior to the NO_x SIP Call (1988–1999). We note July O_3 biases of up to +10 to +30 ppb over all regions in the scatter plots of monthly mean MDA8 O_3 and monthly mean T_{max} (Figure 4a, d, and g). Summertime O_3 biases over the eastern US have been noted in previous global and regional modeling studies (Fiore et al., 2009; Nolte et al., 2008; Reidmiller et al., 2009). The range of modeled monthly mean T_{max} is also greater than that of the CASTNet in both the Great Lakes and the Mid-Atlantic, with some months exceeding the warmest observed T_{max} by over 5 K. At monthly mean temperatures above 305 K produced by the model, simulated MDA8 O_3 ceases to respond linearly to increasing T_{max} (Figures 4d, g). These plateaus in MDA8 O_3 may be reflective of the known decreasing lifetime of PAN at incrementally higher temperatures (e.g. Steiner et al., 2010). This saturation effect manifests in the low correlations and slopes noted below for the model.

Over the Northeast and the Great Lakes, the model reproduces the observed correlation coefficients (Figure 4b, h) and $m_{O3\text{-}T}$ (Figure 4c, i) throughout the year. In the Mid-Atlantic, the AM3 reproduces $m_{O3\text{-}T}$ in the winter and early spring and simulates the observed summertime decrease in O_3-temperature correlations, but correlations are excessively weak (July CASTNet: r = 0.4; model: r = 0.0; Figure 4e). Additionally, the model underestimates $m_{O3\text{-}T}$ in late summer and autumn by as much as 3 ppb K^{-1} (Figure 4f). The cause of these results may again point to PAN saturation occurring for high modeled temperatures.

Ideally the model should capture both spatial and climatic variability in MDA8 O_3 and T_{max}, as discussed in Sect. 3 we are interested in separating temporal and spatial variability to isolate the response of MDA8 O_3 to year-to-year fluctuations in monthly average T_{max} from regional differences in precursor emissions and the photochemical regime. We note that although precursor emissions may vary interannually, most of our model emissions do not (only isoprene and lightning NO_x are tied to the model meteorology). We average over all data modeled at CASTNet site locations within each region and present these regional climatologies in Figure 6. Despite up to a +10 to +20 ppb O_3 bias, the model captures $m_{O3\text{-}T}$ over the Northeast, and with the exception of the timing of the highest $m_{O3\text{-}T}$ occurring one month early in the model, the seasonality of $m_{O3\text{-}T}$ over the Northeast is generally well simulated (Figure 6c). Values of $m_{O3\text{-}T}$ are also well reproduced in the winter and early spring over the Mid-Atlantic (Figure 6f) and the Great Lakes (Figure 6i), but are lower by roughly 2–4 ppb K^{-1} in the Mid-Atlantic and 1–2 ppb K^{-1} in the Great Lakes in the summer (consistent with Figures 2d and 3d over the Mid-Atlantic) and early autumn. For comparison, the dashed lines in Figure 6 are monthly values of $m_{O3\text{-}T}$ calculated using the methodology from Figure 4, but extended to the full record length. In the Northeast, we find that the model represents both the spatial gradients across O_3 and temperature (Figure 4a-c) as well as the role of year-to-year weather changes on O_3 (Figure 6a-c). Whereas spatial gradients of O_3 and temperature over the Mid-Atlantic and Great Lakes are well captured by the model (Figure 4), in these regions the response of O_3 to year-to-year fluctuations in temperature is only weakly reproduced. We find that over these same two regions, monthly mean T_{max} is at times 5 K too warm with respect to the CASTNet sites (Figure 6d, g). When the modeled monthly mean temperatures that are above the warmest observed monthly mean T_{max} are removed from the data (not shown) over the Mid-Atlantic, a sensitivity of 2.5 ppb K^{-1} is

calculated for July (r = 0.7). Additional increases in O_3-temperature sensitivities of 0.5 ppb K^{-1} in the summer months occurs over the Great Lakes when temperatures above 305 K are excluded.

Fundamentally different meteorological processes modulate O_3 levels in the southern and the northern regions of the eastern US (Camalier et al., 2007). Migratory high-pressure systems strongly influence summer O_3 variability over this domain, except in the south where the stagnant Bermuda high-pressure system tends to limit day-to-day changes (Vukovich, 1995). The model best simulates the O_3-temperature relationship over the Northeast and most of the Great Lakes. It is here that summertime pollutant ventilation is known to be driven by northeastward propagating cyclones with associated cold fronts extending south to roughly 35^o N (Leibensperger et al., 2008; Logan, 1989; Vukovich, 1995); below this latitude, both deep convection and inflow from the Gulf of Mexico have been identified as the dominant pollutant ventilation mechanisms (Li et al., 2005). The better represented O_3-temperature relationships north versus south of 35^o N may indirectly confirm model skill at resolving synoptic scale meteorological systems. In contrast, the lack of skill in the Mid-Atlantic region may point to inadequate representation of both regional circulation and convective ventilation, a notorious problem for global climate models.

Stronger linear dependence on humidity rather than temperature in the southern US has also been noted (Camalier et al., 2007; Dawson et al., 2007; Davis et al., 2011). Davis et al. (2011) found the regional model, Community Multiscale Air Quality (CMAQ), to underestimate this predominantly inverse relationship between O_3 and relative humidity over the Mid-Atlantic. A similar problem could be limiting the success of the GFDL AM3 CCM to reproduce observed O_3 levels in this region, though the observed effects of humidity on O_3 have varying sign and have been perceived as slight in comparison to that of temperature (Jacob and Winner, 2009).

5. Estimating the impact of model biases in T_{max} on MDA8 O_3.

Excess summertime surface O_3 formation in the eastern US is a pervasive problem in gridded global (Fiore et al., 2009; Murazaki and Hess, 2006; Reidmiller et al., 2009) and regional (Nolte et al., 2008) models and raises questions about the accuracy of their estimates of future O_3

concentrations. Here, we use the O_3-temperature relationship derived from observations (conservatively estimating a 3 ppb K^{-1} sensitivity; Figures 4c, f, i and 6c, f, i), to investigate the potential contribution of model temperature biases to excess surface O_3 over our study domain. To evaluate modeled T_{max} biases where CASTNet sites do not exist, we utilize 20 years of monthly mean T_{max} from two independent gridded datasets: The University of Washington (UW) (Maurer et al., 2002) and the North American Regional Reanalysis (NARR) (Mesinger et al., 2006). The UW data are hourly observations from the National Oceanic and Atmospheric Administration /National Climatic Data Center Co-op stations spatially interpolated and gridded to $1/8^o$ x $1/8^o$ horizontal resolution. The NARR data are the product of assimilating the NCEP /Department of Energy global reanalysis (Kanamitsu et al., 2002) with a version of the NCEP Eta model at 32 km x 32 km horizontal resolution.

The estimated simulated summer MDA8 O_3 associated with the model T_{max} bias is shown in Figure 7. Both the NARR and the UW indicate that temperature is not a factor in excess O_3 production in June in the eastern US, but they disagree in July. The UW data suggest the GFDL AM3 CCM is too cool in this month, yet both the NARR and the CASTNet observations suggest the opposite. The NARR output is 3-hourly while the UW data are calculated from hourly data, so NARR should be inherently cooler than UW; we suggest this discrepancy between the datasets requires additional study.

Given the general rural location of CASTNet sites in the otherwise heavily urbanized eastern US, they may be biased cool (relative to a regional average). Nonetheless, we find the largest modeled summer T_{max} biases to occur over the Great Lakes and the Mid-Atlantic. Figure 7 indicates that positive modeled temperature biases for the months of August and September over these same regions are a possible source of up to 10–15 ppb of the excess modeled O_3, ~30–50% of the O_3 bias in some grid boxes. We note that because the modeled regional O_3 sensitivities to T_{max} in the summer over both the Mid-Atlantic and the Great Lakes are underestimated in the model (Figure 6f, i), we consider these estimates as an upper limit to the contribution of temperature biases to the O_3 bias (using the modeled $m_{O3\text{-}T}$ of 2 ppb K^{-1} would lower our estimate to 6–10 ppb). Clearly, excessively warm temperatures cannot be the only factor contributing to the model O_3 bias as +30 ppb biases occur over some areas with well simulated T_{max}, particularly

461 in the Mid-Atlantic. For example, modeled O_3 production over some areas of the Mid-Atlantic
462 region is highly sensitive to the treatment of isoprene nitrate ($RONO_2$) chemistry (e.g. whether
463 isoprene nitrates represent a terminal or interim sink for NO_x) (Fiore et al., 2005; Horowitz et al.,
464 2007; Ito et al., 2009; Wu et al., 2007).
465
466 **6. Conclusion.**
467
468 Our study characterizes climatological O_3-temperature relationships from long-term observations
469 over the eastern US for the purpose of evaluating chemistry-climate models (CCMs) that are
470 used to project future air quality. We consider temperature as a proxy to synthesize the complex
471 effects of several temperature-dependent meteorological and chemical processes influencing O_3
472 concentrations. We report the slope of the O_3-temperature relationship, $m_{O3\text{-}T}$, at both site-level
473 and regional scales, as derived from monthly mean daily maximum temperatures (T_{max}) and
474 monthly mean daily maximum 8-hour average (MDA8) O_3 concentrations. By segregating the
475 observations into two time periods (1988–1999 and 2000–2009), we confirm the previously
476 noted ~ 1 ppb K^{-1} regional decrease in $m_{O3\text{-}T}$ between these periods attributed to power plant NO_x
477 emission reductions (Bloomer et al., 2009).
478
479 Our evaluation of the GFDL AM3 CCM shows modeled MDA8 O_3 biases in summer (ranging
480 from +10 to +20 ppb in the Northeast and +10 to +30 ppb in the Great Lakes and Mid-Atlantic).
481 Simulated monthly mean T_{max} is at times 5 K too warm with respect to observations in the latter
482 two regions. Despite these biases, GFDL AM3 reproduces the general spatial and temporal
483 characteristics of $m_{O3\text{-}T}$ and associated correlation coefficients O_3 in the Northeast, although it
484 underestimates $m_{O3\text{-}T}$ by 2–4 ppb K^{-1} in the summer over the Mid-Atlantic, where simulated
485 correlation coefficients are excessively weak.
486
487 The skill of the model in the northern half of study domain may derive from the ability of the
488 GFDL AM3 CCM to simulate the fundamental meteorological and chemical processes that
489 modulate the surface O_3 response to temperature. These processes include stagnation and
490 ventilation events resulting from migrating synoptic systems across the eastern US (Logan, 1989;
491 Vukovich, 1995; Leibensperger et al., 2008). By contrast, poorer representation of O_3-

492 temperature relationships in the mid-Atlantic may reflect inadequate representation of
493 convection and inflow from the Gulf of Mexico (Li et al., 2005).
494
495 We illustrate how the observationally derived O_3-temperature relationships can be applied to
496 estimate the contribution of modeled temperature biases to excess surface O_3 over our study
497 domain. In order to assess model temperature biases over the full domain (rather than solely in
498 the limited locations of the CASTNet sites), we evaluate model T_{max} with two gridded data sets,
499 both of which suggest summer T_{max} biases of up to 5 K in August and September for the Mid-
500 Atlantic and the Great Lakes. Multiplying these modeled T_{max} biases by our observation-based
501 O_3 sensitivity of 3 ppb K^{-1}, we estimate a maximum contribution of 10–15 ppb O_3 from
502 simulated T_{max} biases, and conclude they are not the major driver of the large-scale O_3 bias.
503
504 The larger standard errors in $m_{O3\text{-}T}$ calculated from the regionally averaged observed data (Figure
505 6) as compared to regional $m_{O3\text{-}T}$ constructed from monthly data at each site (Figure 4) highlights
506 the need for longer data records to improve statistical power and better quantify robust
507 relationships between MDA8 O_3 and T_{max}. As such, we stress the importance of continuing to
508 maintain long-term, quality controlled, co-located meteorology and air quality measurement
509 networks in the eastern US such as that of the CASTNet, for their crucial importance in
510 documenting relationships and trends therein. Observation-based relationships should provide
511 key constraints to evaluate CCM skill at resolving processes relevant to project accurately the
512 response of air quality to future changes in climate.
513
514 **Acknowledgements.**
515
516 We would like to thank Bryan Bloomer (U.S. EPA), Hiram Levy II (GFDL/NOAA), and Allison
517 Steiner (University of Michigan – Ann Arbor) for their helpful comments and discussion. We
518 also gratefully acknowledge help from both Jenise Swall and Steve Howard (U.S. EPA) for
519 processing of the CASTNet data. Assistance with NARR data handling was provided by
520 Christopher Kerr (GFDL/NOAA).
521
522 **References.**

523

524 Austin, J., Wilson, R.J., 2006. Ensemble simulations of the decline and recovery of stratospheric
525 ozone. J Geophys Res-Atmos 111, -.

526 Aw, J., Kleeman, M.J., 2003. Evaluating the first-order effect of intraannual temperature
527 variability on urban air pollution. J. Geophys. Res. 108, 4365.

528 Ayers, G.P., 2001. Comment on regression analysis of air quality data. Atmospheric
529 Environment 35, 2423-2425.

530 Bernard, S.M., Samet, J.M., Grambsch, A., Ebi, K.L., Romieu, I., 2001. The potential impacts of
531 climate variability and change on air pollution-related health effects in the United States. Environ
532 Health Persp 109, 199-209.

533 Bloomer, B.J., Stehr, J.W., Piety, C.A., Salawitch, R.J., Dickerson, R.R., 2009. Observed
534 relationships of ozone air pollution with temperature and emissions. Geophys. Res. Lett. 36,
535 L09803.

536 Bloomer, B.J., Vinnikov, K.Y., Dickerson, R.R., 2010. Changes in seasonal and diurnal cycles of
537 ozone and temperature in the eastern US. Atmospheric Environment 44, 2543-2551.

538 Brühl, C., Crutzen, P.J., 1988. Scenarios of possible changes in atmospheric temperatures and
539 ozone concentrations due to man's activities, estimated with a one-dimensional coupled
540 photochemical climate model. Clim Dynam 2, 173-203.

541 Camalier, L., Cox, W., Dolwick, P., 2007. The effects of meteorology on ozone in urban areas
542 and their use in assessing ozone trends. Atmospheric Environment 41, 7127-7137.

543 Cantrell, C.A., 2008. Technical Note: Review of methods for linear least-squares fitting of data
544 and application to atmospheric chemistry problems. Atmos. Chem. Phys. 8, 5477-5487.

545 Cardelino, C.A., Chameides, W.L., 1990. Natural Hydrocarbons, Urbanization, and Urban
546 Ozone. J Geophys Res-Atmos 95, 13971-13979.

547 Chan, E., 2009. Regional ground-level ozone trends in the context of meteorological influences
548 across Canada and the eastern United States from 1997 to 2006. J Geophys Res-Atmos 114, -.

549 Christensen, J.H., Hewitson, B., Busuioc, A., Chen, A., Gao, X., Held, I., Jones, R., Kolli, R.K.,
550 Kwon, W.-T., Laprise, R., Rueda, V.M., Mearns, L., Menéndez, C.G., Räisänen, J., Rinke, A.,
551 Sarr, A., Whetton, P., 2007. Regional Climate Projections. In: Climate Change 2007:The
552 Physical Science Basis. Contribution of Working Group I to the Fourth Assessment Report of the
553 Intergovernmental Panel on Climate Change. Cambridge University Press, Cambridge, United
554 Kingdom and New York, NY, USA.

555 Clark, T.L., Karl, T.R., 1982. Application of Prognostic Meteorological Variables to Forecasts of
556 Daily Maximum One-Hour Ozone Concentrations in the Northeastern United States. Journal of
557 Applied Meteorology 21, 1662-1671.

558 Clarke, J.F., Edgerton, E.S., Martin, B.E., 1997. Dry deposition calculations for the clean air
559 status and trends network. Atmospheric Environment 31, 3667-3678.

560 Davis, J., Cox, W., Reff, A., Dolwick, P., 2011. A comparison of CMAQ-based and observation-
561 based statistical models relating ozone to meteorological parameters. Atmospheric Environment
562 45, 3481-3487.

563 Davis, J.C., 1986. Statistics and data analysis in geology, 2nd ed. Wiley, New York.

564 Dawson, J.P., Adams, P.J., Pandis, S.N., 2007. Sensitivity of ozone to summertime climate in the
565 eastern USA: A modeling case study. Atmospheric Environment 41, 1494-1511.

566 Donner, L.J., Wyman, B.L., Hemler, R.S., Horowitz, L.W., Ming, Y., Zhao, M., Golaz, J.-C.,
567 Ginoux, P., Lin, S.J., Schwarzkopf, M.D., Austin, J., Alaka, G., Cooke, W.F., Delworth, T.L.,
568 Freidenreich, S.M., Gordon, C.T., Griffies, S.M., Held, I.M., Hurlin, W.J., Klein, S.A., Knutson,
569 T.R., Langenhorst, A.R., Lee, H.-C., Lin, Y., Magi, B.I., Malyshev, S.L., Milly, P.C.D., Naik,
570 V., Nath, M.J., Pincus, R., Ploshay, J.J., Ramaswamy, V., Seman, C.J., Shevliakova, E., Sirutis,
571 J.J., Stern, W.F., Stouffer, R.J., Wilson, R.J., Winton, M., Wittenberg, A.T., Zeng, F., 2011. The
572 Dynamical Core, Physical Parameterizations, and Basic Simulation Characteristics of the
573 Atmospheric Component AM3 of the GFDL Global Coupled Model CM3. J Climate 24, 3484-
574 3519.

575 Eder, B.K., Davis, J.M., Bloomfield, P., 1993. A characterization of the spatiotemporal
576 variability of non-urban ozone concentrations over the eastern United States. Atmospheric
577 Environment. Part A. General Topics 27, 2645-2668.

578 Emmons, L.K., Walters, S., Hess, P.G., Lamarque, J.F., Pfister, G.G., Fillmore, D., Granier, C.,
579 Guenther, A., Kinnison, D., Laepple, T., Orlando, J., Tie, X., Tyndall, G., Wiedinmyer, C.,
580 Baughcum, S.L., Kloster, S., 2010. Description and evaluation of the Model for Ozone and
581 Related chemical Tracers, version 4 (MOZART-4). Geosci. Model Dev. 3, 43-67.

582 Fiore, A.M., Dentener, F.J., Wild, O., Cuvelier, C., Schultz, M.G., Hess, P., Textor, C., Schulz,
583 M., Doherty, R.M., Horowitz, L.W., MacKenzie, I.A., Sanderson, M.G., Shindell, D.T.,
584 Stevenson, D.S., Szopa, S., Van Dingenen, R., Zeng, G., Atherton, C., Bergmann, D., Bey, I.,
585 Carmichael, G., Collins, W.J., Duncan, B.N., Faluvegi, G., Folberth, G., Gauss, M., Gong, S.,
586 Hauglustaine, D., Holloway, T., Isaksen, I.S.A., Jacob, D.J., Jonson, J.E., Kaminski, J.W.,
587 Keating, T.J., Lupu, A., Marmer, E., Montanaro, V., Park, R.J., Pitari, G., Pringle, K.J., Pyle,
588 J.A., Schroeder, S., Vivanco, M.G., Wind, P., Wojcik, G., Wu, S., Zuber, A., 2009. Multimodel
589 estimates of intercontinental source-receptor relationships for ozone pollution. J Geophys Res-
590 Atmos 114, -.

591 Fiore, A.M., Horowitz, L.W., Purves, D.W., Levy, H., Evans, M.J., Wang, Y.X., Li, Q.B.,
592 Yantosca, R.M., 2005. Evaluating the contribution of changes in isoprene emissions to surface
593 ozone trends over the eastern United States. J Geophys Res-Atmos 110, -.

594 Fiore, A.M., Jacob, D.J., Mathur, R., Martin, R.V., 2003. Application of empirical orthogonal
595 functions to evaluate ozone simulations with regional and global models. J Geophys Res-Atmos
596 108, -.

Frost, G.J., McKeen, S.A., Trainer, M., Ryerson, T.B., Neuman, J.A., Roberts, J.M., Swanson, A., Holloway, J.S., Sueper, D.T., Fortin, T., Parrish, D.D., Fehsenfeld, F.C., Flocke, F., Peckham, S.E., Grell, G.A., Kowal, D., Cartwright, J., Auerbach, N., Habermann, T., 2006. Effects of changing power plant NOx emissions on ozone in the eastern United States: Proof of concept. J Geophys Res-Atmos 111, -.

Gego, E., Gilliland, A., Godowitch, J., Rao, S.T., Porter, P.S., Hogrefe, C., 2008. Modeling analyses of the effects of changes in nitrogen oxides emissions from the electric power sector on ozone levels in the eastern United States. J Air Waste Manage 58, 580-588.

Gego, E., Porter, P.S., Gilliland, A., Rao, S.T., 2007. Observation-based assessment of the impact of nitrogen oxides emissions reductions on ozone air quality over the eastern United States. J Appl Meteorol Clim 46, 994-1008.

Gilliland, A.B., Hogrefe, C., Pinder, R.W., Godowitch, J.M., Foley, K.L., Rao, S.T., 2008. Dynamic evaluation of regional air quality models: Assessing changes in O-3 stemming from changes in emissions and meteorology. Atmospheric Environment 42, 5110-5123.

Godowitch, J.M., Hogrefe, C., Rao, S.T., 2008. Diagnostic analyses of a regional air quality model: Changes in modeled processes affecting ozone and chemical-transport indicators from NOx point source emission reductions. J Geophys Res-Atmos 113, -.

Guenther, A., Karl, T., Harley, P., Wiedinmyer, C., Palmer, P.I., Geron, C., 2006. Estimates of global terrestrial isoprene emissions using MEGAN (Model of Emissions of Gases and Aerosols from Nature). Atmos. Chem. Phys. 6, 3181-3210.

Guenther, A.B., Zimmerman, P.R., Harley, P.C., Monson, R.K., Fall, R., 1993. Isoprene and Monoterpene Emission Rate Variability - Model Evaluations and Sensitivity Analyses. J Geophys Res-Atmos 98, 12609-12617.

Hogrefe, C., Lynn, B., Civerolo, K., Ku, J.Y., Rosenthal, J., Rosenzweig, C., Goldberg, R., Gaffin, S., Knowlton, K., Kinney, P.L., 2004. Simulating changes in regional air pollution over the eastern United States due to changes in global and regional climate and emissions. J. Geophys. Res. 109, D22301.

Horowitz, L.W., Fiore, A.M., Milly, G.P., Cohen, R.C., Perring, A., Wooldridge, P.J., Hess, P.G., Emmons, L.K., Lamarque, J.F., 2007. Observational constraints on the chemistry of isoprene nitrates over the eastern United States. J Geophys Res-Atmos 112, -.

Horowitz, L.W., Walters, S., Mauzerall, D.L., Emmons, L.K., Rasch, P.J., Granier, C., Tie, X., Lamarque, J.-F., Schultz, M.G., Tyndall, G.S., Orlando, J.J., Brasseur, G.P., 2003. A global simulation of tropospheric ozone and related tracers: Description and evaluation of MOZART, version 2. J. Geophys. Res. 108, 4784.

Ito, A., Sillman, S., Penner, J.E., 2009. Global chemical transport model study of ozone response to changes in chemical kinetics and biogenic volatile organic compounds emissions due to increasing temperatures: Sensitivities to isoprene nitrate chemistry and grid resolution. J. Geophys. Res. 114, D09301.

635 Jacob, D., Horowitz, L.W., Munger, J.W., Heikes, B.G., Dickerson, R.R., Artz, R.S., Keene,
636 W.C., 1995. Seasonal transition from NOx- to hydrocarbon-limited conditions for ozone
637 production over the eastern United States in September. J. Geophys. Res. 100, 9315-9324.

638 Jacob, D., Logan, J.A., Yevich, R.M., Gardner, G.M., Spivakovsky, C.M., Wofsy, S.C., Munger,
639 J.W., Sillman, S., Prather, M.J., Rodgers, M.O., Westberg, H., Zimmerman, P.R., 1993.
640 Simulation of Summertime Ozone over North America. J. Geophys. Res. 98, 14797-14816.

641 Jacob, D., Winner, D.A., 2009. Effect of climate change on air quality. Atmospheric
642 Environment 43, 51-63.

643 Kanamitsu, M., Ebisuzaki, W., Woollen, J., Yang, S.K., Hnilo, J.J., Fiorino, M., Potter, G.L.,
644 2002. Ncep-Doe Amip-Ii Reanalysis (R-2). Bulletin of the American Meteorological Society 83,
645 1631-1643.

646 Kleinman, L.I., 1991. Seasonal Dependence of Boundary-Layer Peroxide Concentration - the
647 Low and High Nox Regimes. J Geophys Res-Atmos 96, 20721-20733.

648 Klonecki, A., Levy, H., II, 1997. Tropospheric chemical ozone tendencies in CO-CH4-NOy-
649 H2O system: Their sensitivity to variations in environmental parameters and their application to
650 a global chemistry transport model study. J. Geophys. Res. 102, 21221-21237.

651 Korsog, P.E., Wolff, G.T., 1991. An examination of urban ozone trends in the Northeastern U.S.
652 (1973-1983) using a robust statistical method. Atmospheric Environment. Part B. Urban
653 Atmosphere 25, 47-57.

654 Kunkel, K., Huang, H.C., Liang, X.Z., Lin, J.T., Wuebbles, D., Tao, Z., Williams, A., Caughey,
655 M., Zhu, J., Hayhoe, K., 2008. Sensitivity of future ozone concentrations in the northeast USA to
656 regional climate change. Mitigation and Adaptation Strategies for Global Change 13, 597-606.

657 Lamarque, J.F., Bond, T.C., Eyring, V., Granier, C., Heil, A., Klimont, Z., Lee, D., Liousse, C.,
658 Mieville, A., Owen, B., Schultz, M.G., Shindell, D., Smith, S.J., Stehfest, E., Van Aardenne, J.,
659 Cooper, O.R., Kainuma, M., Mahowald, N., McConnell, J.R., Naik, V., Riahi, K., van Vuuren,
660 D.P., 2010. Historical (1850â€“2000) gridded anthropogenic and biomass burning emissions of
661 reactive gases and aerosols: methodology and application. Atmos. Chem. Phys. 10, 7017-7039.

662 Lamb, B., Guenther, A., Gay, D., Westberg, H., 1987. A national inventory of biogenic
663 hydrocarbon emissions. Atmospheric Environment (1967) 21, 1695-1705.

664 Lawrence, P.J., Chase, T.N., 2007. Representing a new MODIS consistent land surface in the
665 Community Land Model (CLM 3.0). J. Geophys. Res. 112, G01023.

666 Lehman, J., Swinton, K., Bortnick, S., Hamilton, C., Baldridge, E., Eder, B., Cox, B., 2004.
667 Spatio-temporal characterization of tropospheric ozone across the eastern United States.
668 Atmospheric Environment 38, 4357-4369.

669 Leibensperger, E.M., Mickley, L.J., Jacob, D.J., 2008. Sensitivity of US air quality to mid-
670 latitude cyclone frequency and implications of 1980-2006 climate change. Atmos Chem Phys 8,
671 7075-7086.

672 Levy, J.I., Carrothers, T.J., Tuomisto, J.T., Hammitt, J.K., Evans, J.S., 2001. Assessing the
673 public health benefits of reduced ozone concentrations. Environ Health Persp 109, 1215-1226.

674 Li, Q.B., Jacob, D.J., Park, R., Wang, Y.X., Heald, C.L., Hudman, R., Yantosca, R.M., Martin,
675 R.V., Evans, M., 2005. North American pollution outflow and the trapping of convectively lifted
676 pollution by upper-level anticyclone. J Geophys Res-Atmos 110, -.

677 Lin, C.Y.C., Jacob, D.J., Fiore, A.M., 2001. Trends in exceedances of the ozone air quality
678 standard in the continental United States, 1980-1998. Atmospheric Environment 35, 3217-3228.

679 Lin, X., Trainer, M., Liu, S.C., 1988. On the Nonlinearity of the Tropospheric Ozone Production.
680 J Geophys Res-Atmos 93, 15879-15888.

681 Logan, J.A., 1983. Nitrogen Oxides in the Troposphere: Global and Regional Budgets. J.
682 Geophys. Res. 88, 10785-10807.

683 Logan, J.A., 1989. Ozone in Rural-Areas of the United-States. J Geophys Res-Atmos 94, 8511-
684 8532.

685 Mahmud, A., Tyree, M., Cayan, D., Motallebi, N., Kleeman, M.J., 2008. Statistical downscaling
686 of climate change impacts on ozone concentrations in California. J. Geophys. Res. 113, D21103.

687 Maurer, E.P., Wood, A.W., Adam, J.C., Lettenmaier, D.P., Nijssen, B., 2002. A long-term
688 hydrologically based dataset of land surface fluxes and states for the conterminous United States.
689 J Climate 15, 3237-3251.

690 Meinshausen, M., Smith, S., Calvin, K., Daniel, J.S., Kainuma, M.L.T., Lamarque, J.-F.,
691 Matsumoto, K., Montzka, S.A., Raper, S.C.B., Riahi, K., Thomson, A.M., Velders, G.J.M., van
692 Vuuren, D., 2011. The RCP Greenhouse Gas Concentrations and their Extension from 1765 to
693 2300. Climate Change.

694 Meleux, F., Solmon, F., Giorgi, F., 2007. Increase in summer European ozone amounts due to
695 climate change. Atmospheric Environment 41, 7577-7587.

696 Mesinger, F., DiMego, G., Kalnay, E., Mitchell, K., Shafran, P.C., Ebisuzaki, W., JoviÄ‡, D.a.,
697 Woollen, J., Rogers, E., Berbery, E.H., Ek, M.B., Fan, Y., Grumbine, R., Higgins, W., Li, H.,
698 Lin, Y., Manikin, G., Parrish, D., Shi, W., 2006. North American Regional Reanalysis. Bulletin
699 of the American Meteorological Society 87, 343-360.

700 Murazaki, K., Hess, P., 2006. How does climate change contribute to surface ozone change over
701 the United States? J Geophys Res-Atmos 111, -.

National Research Council (U.S.). Committee on Tropospheric Ozone Formation and Measurement., 1991. Rethinking the ozone problem in urban and regional air pollution. National Academy Press, Washington, D.C.

Nolte, C.G., Gilliland, A.B., Hogrefe, C., Mickley, L.J., 2008. Linking global to regional models to assess future climate impacts on surface ozone levels in the United States. J Geophys Res-Atmos 113, -.

Olszyna, K.J., Luria, M., Meagher, J.F., 1997. The correlation of temperature and rural ozone levels in southeastern USA. Atmospheric Environment 31, 3011-3022.

Putman, W.M., Lin, S.-J., 2007. Finite-volume transport on various cubed-sphere grids. Journal of Computational Physics 227, 55-78.

Racherla, P.N., Adams, P.J., 2006. Sensitivity of global tropospheric ozone and fine particulate matter concentrations to climate change. J Geophys Res-Atmos 111, -.

Rao, S.T., Ku, J.Y., Berman, S., Zhang, K.S., Mao, H.T., 2003. Summertime characteristics of the atmospheric boundary layer and relationships to ozone levels over the eastern United States. Pure Appl Geophys 160, 21-55.

Rayner, N.A., Parker, D.E., Horton, E.B., Folland, C.K., Alexander, L.V., Rowell, D.P., Kent, E.C., Kaplan, A., 2003. Global analyses of sea surface temperature, sea ice, and night marine air temperature since the late nineteenth century. J. Geophys. Res. 108, 4407.

Reidmiller, D.R., Fiore, A.M., Jaffe, D.A., Bergmann, D., Cuvelier, C., Dentener, F.J., Duncan, B.N., Folberth, G., Gauss, M., Gong, S., Hess, P., Jonson, J.E., Keating, T., Lupu, A., Marmer, E., Park, R., Schultz, M.G., Shindell, D.T., Szopa, S., Vivanco, M.G., Wild, O., Zuber, A., 2009. The influence of foreign vs. North American emissions on surface ozone in the US. Atmos. Chem. Phys. 9, 5027-5042.

Sheffield, J., Goteti, G., Wood, E.F., 2006. Development of a 50-Year High-Resolution Global Dataset of Meteorological Forcings for Land Surface Modeling. Journal of Climate 19, 3088-3111.

Shevliakova, E., Pacala, S.W., Malyshev, S., Hurtt, G.C., Milly, P.C.D., Caspersen, J.P., Sentman, L.T., Fisk, J.P., Wirth, C., Crevoisier, C., 2009. Carbon cycling under 300 years of land use change: Importance of the secondary vegetation sink. Global Biogeochem Cy 23, -.

Sillman, S., Samson, P.J., 1995. Impact of temperature on oxidant photochemistry in urban, polluted rural and remote environments. J. Geophys. Res. 100, 11497-11508.

Steiner, A.L., Davis, A.J., Sillman, S., Owen, R.C., Michalak, A.M., Fiore, A.M., 2010. Observed suppression of ozone formation at extremely high temperatures due to chemical and biophysical feedbacks. P Natl Acad Sci USA 107, 19685-19690.

Steiner, A.L., Tonse, S., Cohen, R.C., Goldstein, A.H., Harley, R.A., 2006. Influence of future climate and emissions on regional air quality in California. J. Geophys. Res. 111, D18303.

738 Vukovich, F.M., 1995. Regional-Scale Boundary-Layer Ozone Variations in the Eastern United-
739 States and Their Association with Meteorological Variations. Atmospheric Environment 29,
740 2259-2273.

741 Weaver, C.P., Cooter, E., Gilliam, R., Gilliland, A., Grambsch, A., Grano, D., Hemming, B.,
742 Hunt, S.W., Nolte, C., Winner, D.A., Liang, X.Z., Zhu, J., Caughey, M., Kunkel, K., Lin, J.T.,
743 Tao, Z., Williams, A., Wuebbles, D.J., Adams, P.J., Dawson, J.P., Amar, P., He, S., Avise, J.,
744 Chen, J., Cohen, R.C., Goldstein, A.H., Harley, R.A., Steiner, A.L., Tonse, S., Guenther, A.,
745 Lamarque, J.F., Wiedinmyer, C., Gustafson, W.I., Leung, L.R., Hogrefe, C., Huang, H.C., Jacob,
746 D.J., Mickley, L.J., Wu, S., Kinney, P.L., Lamb, B., Larkin, N.K., McKenzie, D., Liao, K.J.,
747 Manomaiphiboon, K., Russell, A.G., Tagaris, E., Lynn, B.H., Mass, C., SalathÃ©, E., O'Neill,
748 S.M., Pandis, S.N., Racherla, P.N., Rosenzweig, C., Woo, J.H., 2009. A Preliminary Synthesis of
749 Modeled Climate Change Impacts on U.S. Regional Ozone Concentrations. Bulletin of the
750 American Meteorological Society 90, 1843-1863.

751 Wilks, D.S., 2006. Statistical methods in the atmospheric sciences, 2nd ed. Academic Press,
752 Amsterdam ; Boston.

753 Wu, S., Mickley, L.J., Jacob, D.J., Logan, J.A., Yantosca, R.M., Rind, D., 2007. Why are there
754 large differences between models in global budgets of tropospheric ozone? J Geophys Res-
755 Atmos 112, -.

756 Wu, S., Mickley, L.J., Leibensperger, E.M., Jacob, D.J., Rind, D., Streets, D.G., 2008. Effects of
757 2000-2050 global change on ozone air quality in the United States. J. Geophys. Res. 113,
758 D06302.

759 Wunderli, S., Gehrig, R., 1991. Influence of Temperature on Formation and Stability of Surface
760 Pan and Ozone - a 2-Year Field-Study in Switzerland. Atmos Environ a-Gen 25, 1599-1608.

761 Yienger, J.J., Levy, H., 1995. Empirical-Model of Global Soil-Biogenic Nox Emissions. J
762 Geophys Res-Atmos 100, 11447-11464.
763
764 **Figures**

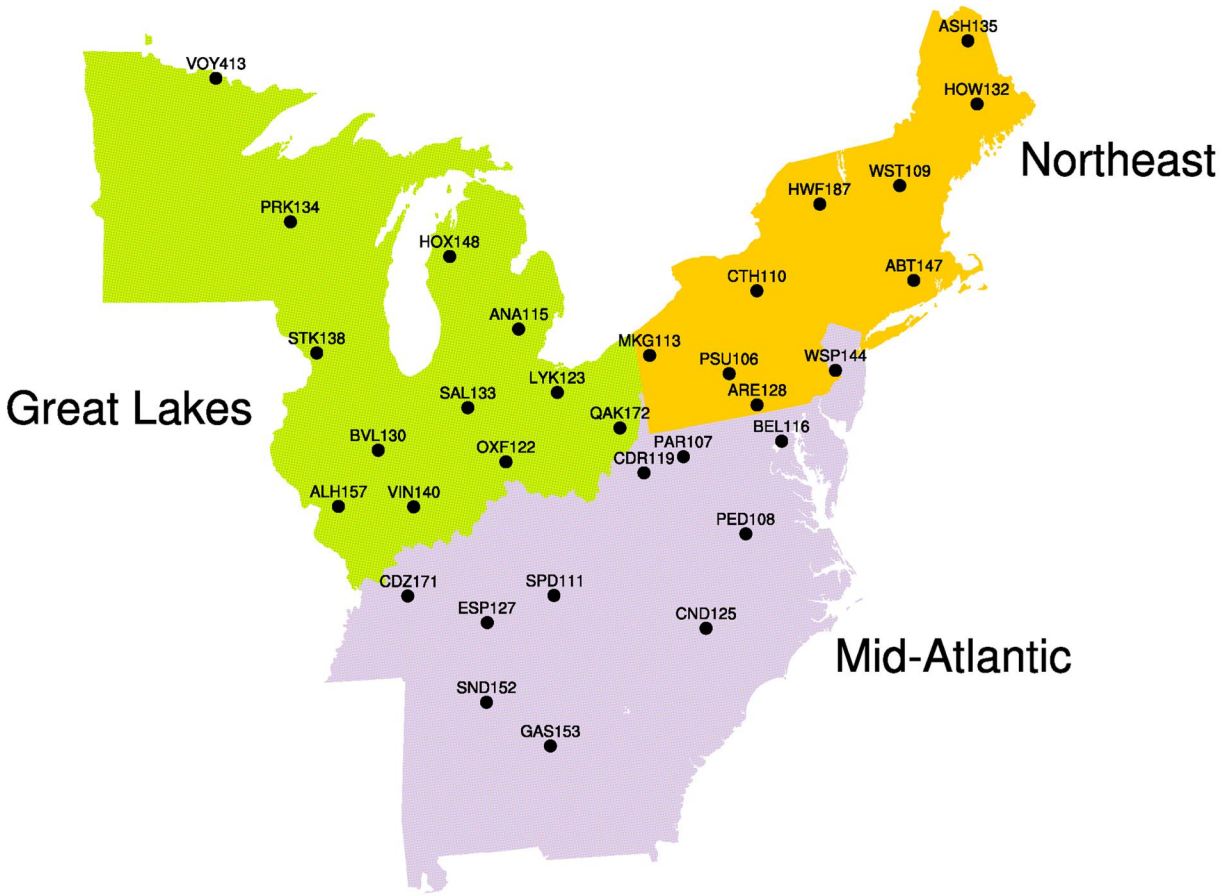

765

766 Figure 1. Geographic locations of CASTNet observation sites in three defined regions in the
767 eastern US: Great Lakes, Northeast, and the Mid-Atlantic where all site selection criteria are met.
768 All sites have at least seven years of data from 1988–2009; all sites reside at elevations greater
769 than 2 meters and less than 600 meters; all sites are at least 50 kilometers from oceanfront; when
770 more than one CASTNet site lies within a model grid box, the site with the longest record is
771 used.

772

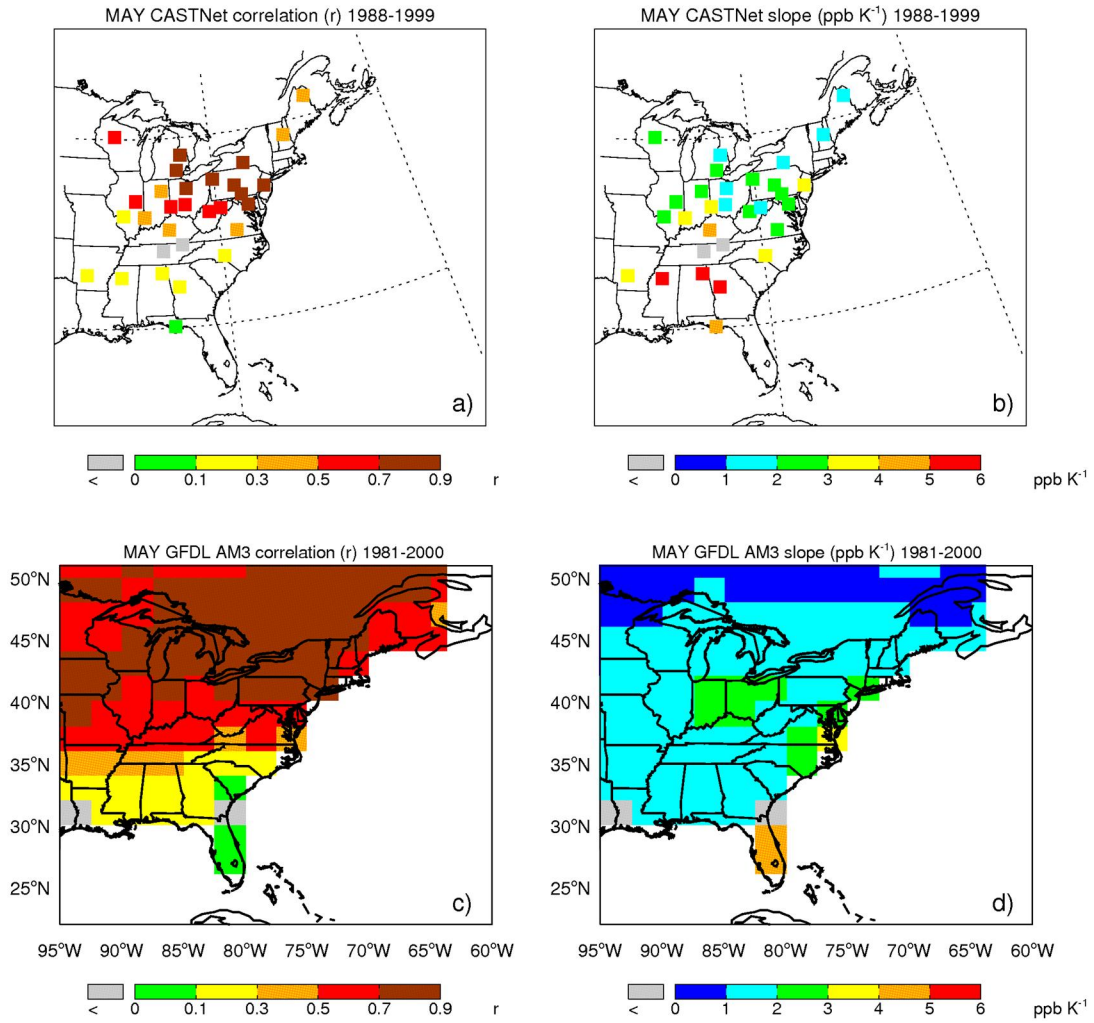

Figure 2. Pearson correlation coefficient (r) of monthly mean surface MDA8 O_3 (ppb) and monthly mean daily maximum surface temperature (K) from a) individual CASTNet sites (1988–1999) and c) in the GFDL AM3 CCM (1981–2000) in May. The slope of the best-fit line between monthly mean MDA8 O_3 and monthly mean daily maximum surface temperature ($m_{O3\text{-}T}$; ppb K^{-1}) from b) individual CASTNet sites and d) in the GFDL AM3 CCM; all CASTNet sites have at least 7 years of data; grey cells denote where $m_{O3\text{-}T}$ minus twice the standard error is less than zero and where modeled $m_{O3\text{-}T}$ less than zero.

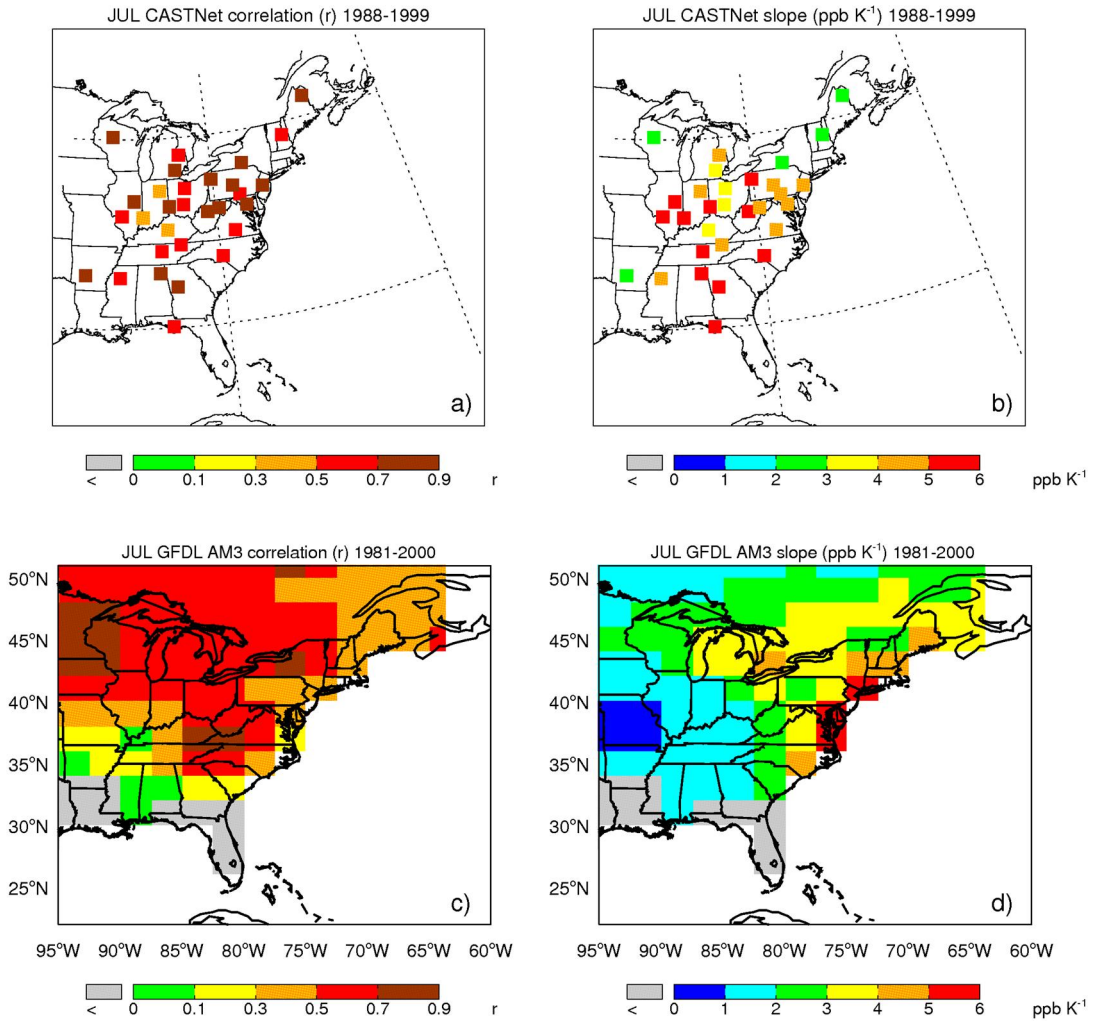

781

782 Figure 3. As for Figure 2, but for July

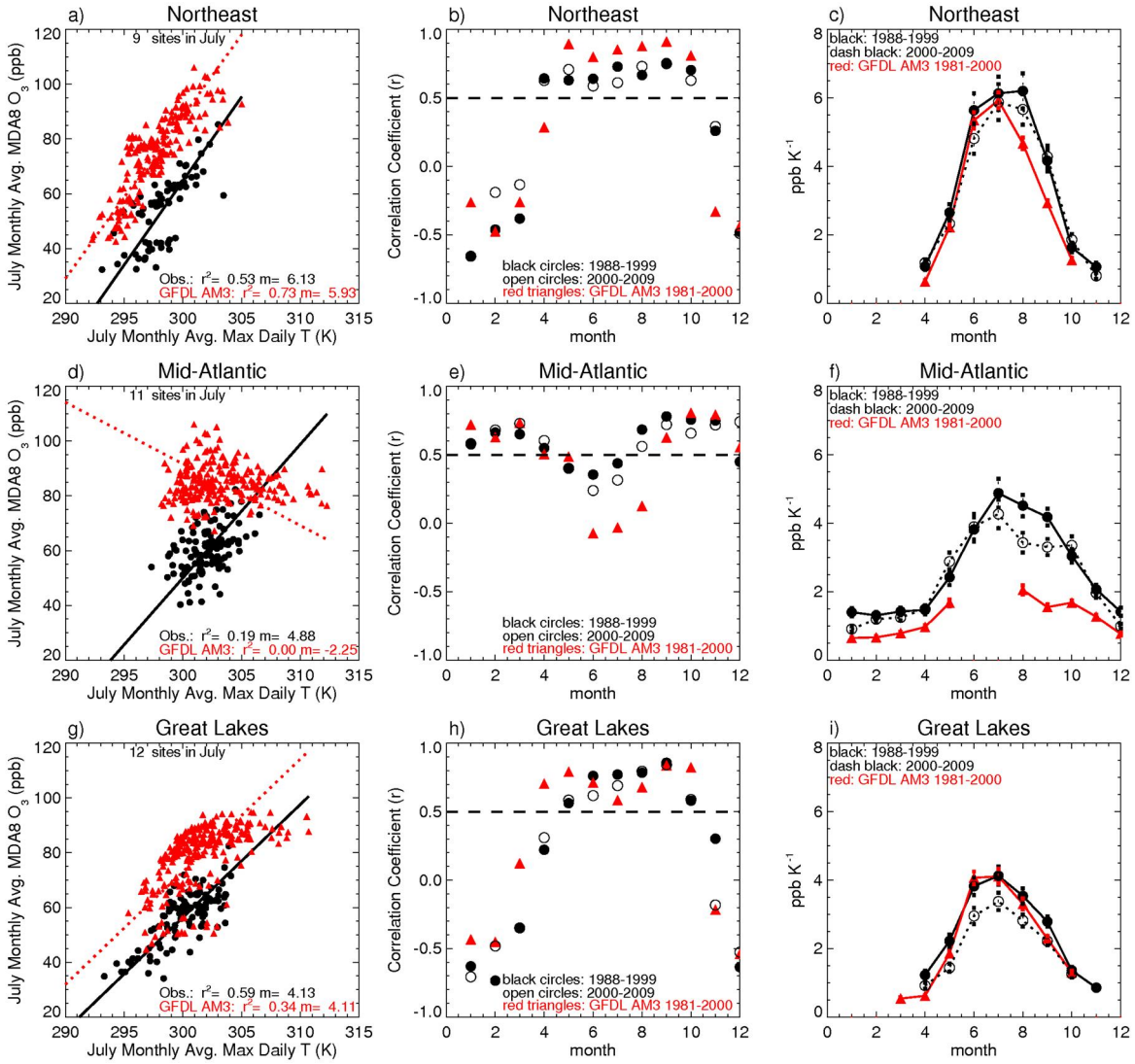

Figure 4. Relationships between monthly mean surface MDA8 O_3 (ppb) and monthly mean daily T_{max} (K) from all CASTNet site locations in each region for 1988–1999 (solid black circles); 2000–2009 (open black circles); and from the GFDL AM3 model for 1981–2000 (red triangles). Scatter plots of July monthly mean MDA8 O_3 concentration (ppb) and July daily T_{max} (K) with linear regression fits (RMA method; Section 2) representing the corresponding $m_{O3\text{-}T}$ (left column). Also shown are monthly values of Pearson correlation coefficients (r ; middle column) and $m_{O3\text{-}T}$ (right column); $m_{O3\text{-}T}$ is not shown for months where $r < 0$; error bars indicate ± 1 standard error on $m_{O3\text{-}T}$ (ppb K^{-1}). The dashed lines at $r = 0.5$ indicate where at least 25% of the variance in the surface O_3 is associated with temperature variability.

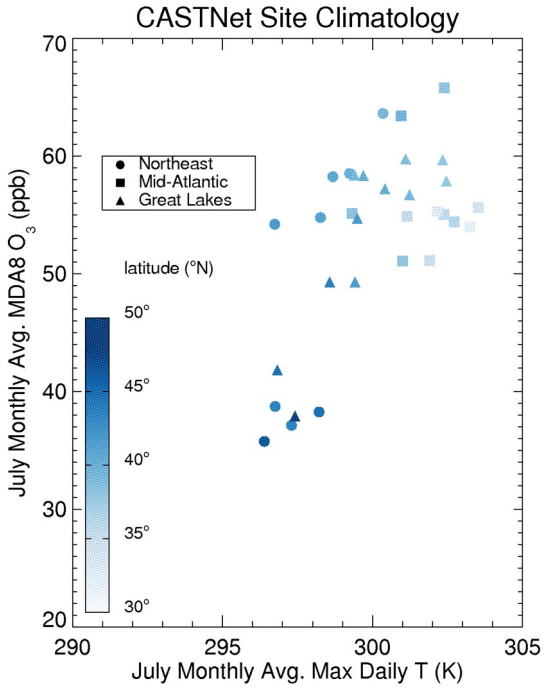

795

796 Figure 5. CASTNet climatology (1988–2009) of July surface MDA8 O_3 (ppb) with July daily
797 maximum temperature (K); each symbol corresponds to each CASTNet site from one of the
798 three regions in Figure 2; circles are Northeast, squares are Mid-Atlantic, and triangles are Great
799 Lakes; shading corresponds to the latitude (^{o}N) of each CASTNet site.

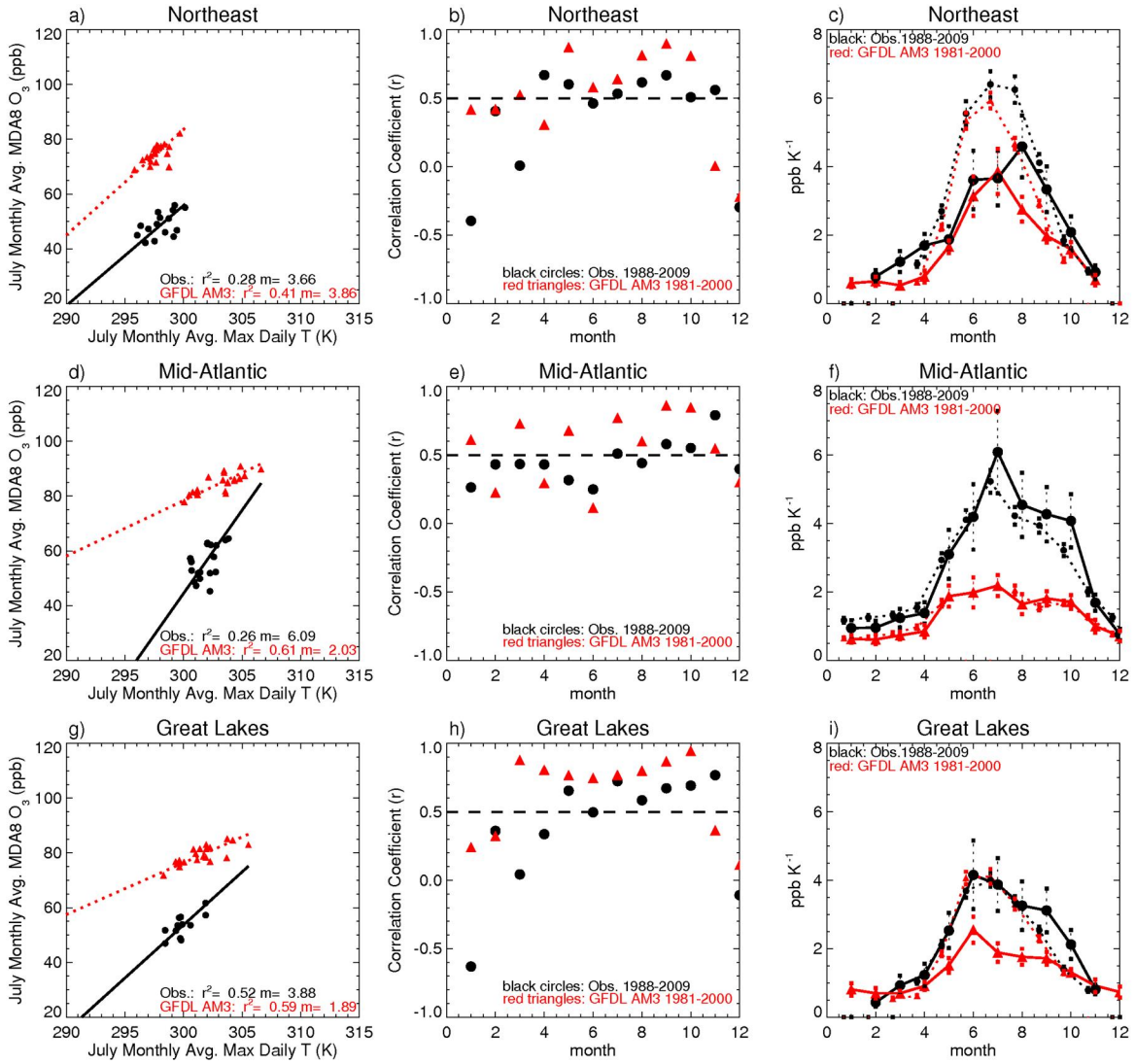

Figure 6. Relationships between monthly regional averages of MDA8 O_3 (ppb) and of daily T_{max} (K) for individual years from 1988 to 2009 (solid black circles) and from the GFDL AM3 model for 1981–2000 (red triangles). For each regional average, we require 75% of all regional sites within a region for the specified month meet the selection criteria (Section 2) . Scatter plots of July monthly mean MDA8 O_3 concentration (ppb) and July daily T_{max} (K) with linear regression fits ($m_{O3\text{-}T}$; left column). Also shown are monthly values of Pearson correlation coefficients (r ; middle column) and $m_{O3\text{-}T}$ (right column); dotted lines use the methodology from Figure 4 but applied to the full 1988-2009 dataset; $m_{O3\text{-}T}$ is not shown for months where $r < 0$; error bars indicate ± 1 standard error on $m_{O3\text{-}T}$ (ppb K^{-1}). The dashed lines at $r = 0.5$ indicate where at least 25% of the variance in the surface O_3 is associated with temperature variability.

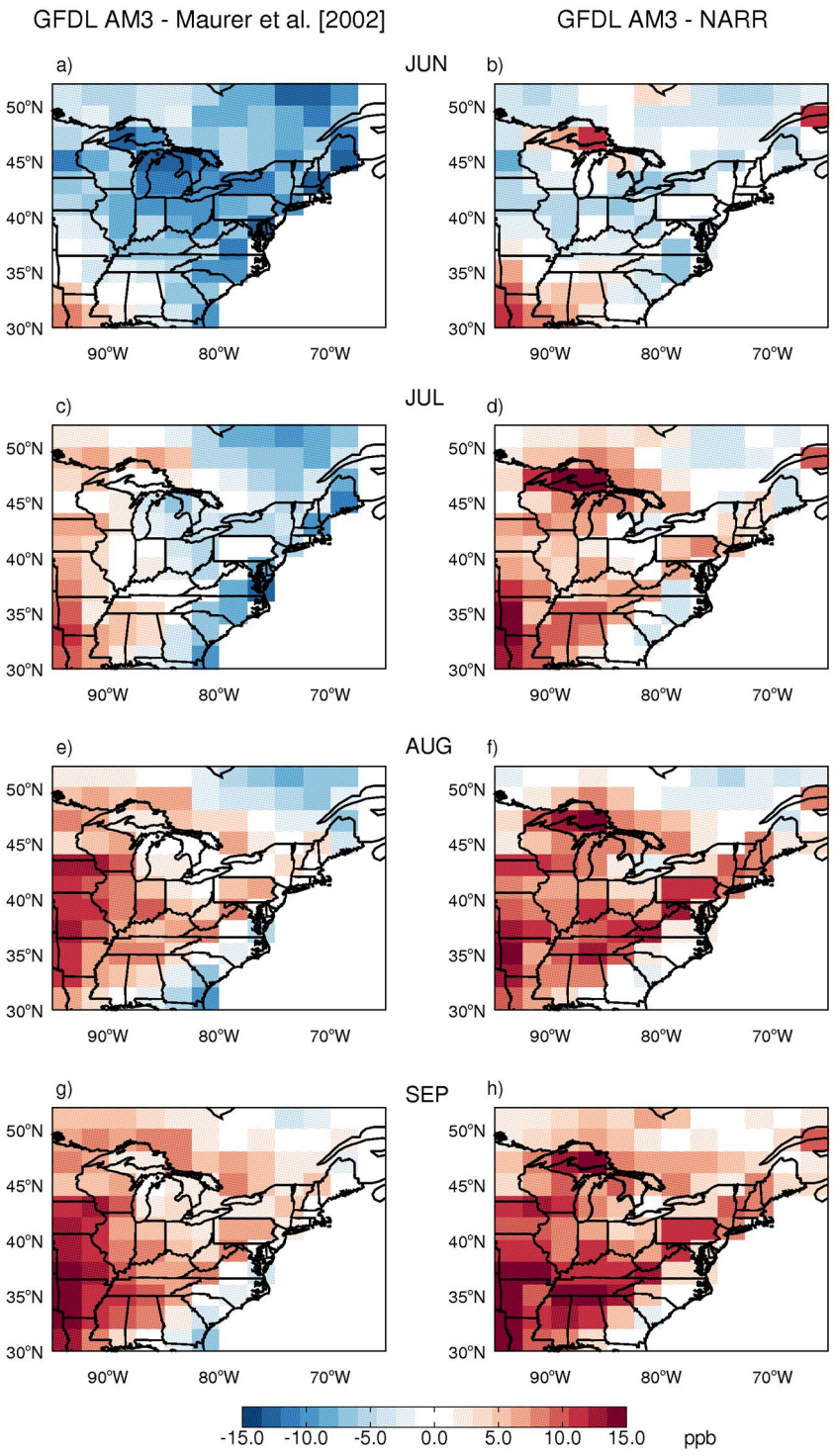

811

812 Figure 7. June, July, August, and September excess modeled O_3 (ppb) attributed to eastern US
813 maximum daily surface temperature biases in the GFDL AM3 CCM; left column uses
814 temperature bias of GFDL AM3 versus *Maurer et al.* [2002]; right column uses bias of GFDL

AM3 versus NARR; temperature biases are multiplied by a conservative, observationally-derived estimate for $m_{O3\text{-}T}$ for 3 ppb K^{-1} over the eastern US (Figures 4 and 6).